View metadata, citation and similar papers at core.ac.uk

Instituto Tecnológico de Aguascalientes

IEEE SECCION AGUASCALIENTES

SEP SECRETARÍA DE EDUCACIÓN PÚBLICA

Home

Call for papers

Important Dates

Paper Submission

Registration

Organizing Committees

Plenary Speakers

Technical Program

Poster Session

Venue

Accomodation

Tourism

Sponsors and Exhibitors

News

Contact us

Gallery

About

# 7th International Conference on Electrical and Electronics Engineering Research

The 7th International Conference on Electrical and Electronics Engineering Research 2010 will take place in the beautiful city of Aguascalientes, located in the heart of Mexico, and it will be held at the Instituto Tecnológico de Aguascalientes, with the support of IEEE Aguascalientes Section, from November 10 -12, 2010.
Technical exchanges within the research community will encompass:

Keynotes
Technical program
Discussion panel
Industrial exposition
Poster session
Student activities
Social and cultural activities

ISBN: 978-607-95060-3-2

provided by Servicio de Coordinación de Bibliotecas de la Universidad Politécnica de Madrid

brought to you by CORE

# Estimation of the rigid transformation between two cameras from the Fundamental Matrix VS from Homographies

L. Pari[1], J.M. Sebastián[2], A. Traslosheros[2], L. Angel[3] and E. Sulla[1]
[1]Departamento Académico de Ingeniería Electrónica, Universidad Nacional de San Agustín
Arequipa, Perú
[2]Departamento de Automática, Ingeniería Electrónica e Informática Industrial (DISAM)
Escuela Técnica Superior de Ingenieros Industriales, Universidad Politécnica de Madrid,España
[3]Facultad de Ingeniería Electrónica, Universidad Pontificia Bolivariana, Bucaramanga, Colombia

*Abstract* — **The 3D reconstruction is an important step for the analytical calculation of the Jacobian of the image in a process of visual control of robots. In a two-camera stereo system that reconstruction depends on the knowledge of the rigid transformation between the two cameras and is represented by the rotation and translation between them. These two parameters are the result of a calibration of the stereo pair, but can also be retrieved from the epipolar geometry of the system, or from a homography obtained by features belonging to a flat object at the scene. In this paper, we make an assessment of the latter two alternatives, taking as reference an Euclidean reconstruction eliminating image distortion. We analyze three cases: the distortion inherent in the camera is corrected, without corrected distortion, and when Gaussian noise is added to the detection of features.**

*Keywords* — **Rigid transformation, fundamental matrix, homography, 3D reconstruction**

## I. Introduction

The three-dimensional reconstruction of the features present in the scene is a necessary process to make visual control which determines the image Jacobian by an analytical calculation [5], resulting in computational cost, increased cycle time control, and availability of accumulating errors. Although the visual control based on the calculation of the Jacobian of the image where is the 3D reconstruction of the point provides good results [2], exists as a conducting online research-based visual control systems are not calibrated [1] [3] [17] based on the properties of epipolar geometry or projective transformations, respectively represented by the fundamental matrix and homography matrix, which ignores the need to calibrate cameras and 3D points reconstructed the scene. In this sense in this paper we study the reconstruction based on parameters obtained from these two matrices.

In a system of two externally uncalibrated cameras, we can recover the rigid transformation (rotation matrix R and translation vector t) between the two chambers from the fundamental matrix or homography based on a [4]. In both cases, recovers only the direction of the translation vector, then it is multiplied by a factor in the case of a homography corresponds to the inverse of the distance between the plane containing the point and origin of the coordinate system of the first camera, while in the case of fundamental matrix comes from its projective nature.

In this paper we discuss two ways to retrieve R t, then with these parameters carried out the 3D reconstruction of the scene points to the cases: when correcting the distortion of the camera itself, without correcting distortion, and when Gaussian noise is added in feature detection. It draws on an Euclidean reconstruction with removal of image distortion, using the method of minimizing the distance between the reprojected rays [13]. The R and t needed to obtain Euclidean reconstruction are obtained by mean of relating the pose (location and orientation) between the patterm and both cameras.

It is known that for a 3D reconstruction [13] Euclidean, it is necessary to have the projection matrix P for each camera, it depends on the matrix of intrinsic parameters and extrinsic (R t). It can also perform a projective reconstruction that explicitly depend on the fundamental matrix F [16], in this case is no longer necessary intrinsic parameters matrix or extrinsic parameters. In this paper we consider an intermediate term, needing to rebuild the matrix of intrinsic parameters only, while the rotation R and translation t are recovered either from the fundamental matrix [10] or from a homography [6 ] [15] [20].

This article is organized as follows: After this introduction, section II describes the recovery of the rotation and translation from the fundamental matrix, while in Section III the recovery of these parameters from a homography. The equipment used, tests and results are shown in Sections IV and V respectively, while in Section VI conclusions are reported and future work.

## II. Retrieving **R** and **t** from the Fundamental Matrix

In a system of two cameras, the projections in both images $\mathbf{m} = [u, v]^T$ and $\mathbf{m}' = [u', v']^T$ (Side coordinates of the image) of a 3D point, are related by the epipolar constraint equation:

$$\tilde{\mathbf{m}}'^T \mathbf{F} \tilde{\mathbf{m}} = 0 \qquad (1)$$

where the characteristics are expressed in projective notation (~), and F is a 3x3 matrix known as the fundamental matrix, which encapsulates all the information of correspondence between $\mathbf{m}$ and $\mathbf{m}'$ its determination is known as projective calibration or calibration weak [8] [12 ]. The estimation of the fundamental matrix has been widely studied research topic mainly in the 90s, existing linear methods, nonlinear and robust [19].

ISBN: 978-607-95060-3-2
Supported by the IEEE Aguascalientes Section and the Instituto Tecnologico de Aguascalientes

Assuming that the intrinsic parameter matrix is known, the essential matrix **E** of the system from the fundamental matrix can be calculated with the following relationship:

$$\mathbf{F} = \mathbf{K}'^{-T}\mathbf{E}\mathbf{K}^{-1} \tag{2}$$

where **K**' y **K** are intrinsic parameter matrices of the second and first camera respectively.

Once the essential matrix **E** is calculated, and knowing that $\mathbf{E} = [\mathbf{t}_x]\mathbf{R}$ [7], where $[t_x]$ is the skew symmetric matrix of t, one can extract the rotation **R** and scaled translation t according to the method proposed by Hartley in [10] based on properties SVD singular decomposition of **E**. By this method there are four possible solutions of the type (**R** | **t** *):

$$\begin{aligned} &(\mathbf{U}\mathbf{W}\mathbf{V}^T \mid \alpha\mathbf{u}_3) \\ &(\mathbf{U}\mathbf{W}\mathbf{V}^T \mid -\alpha\mathbf{u}_3) \\ &(\mathbf{U}\mathbf{W}^T\mathbf{V}^T \mid \alpha\mathbf{u}_3) \\ &(\mathbf{U}\mathbf{W}^T\mathbf{V}^T \mid -\alpha\mathbf{u}_3) \end{aligned} \tag{3}$$

Where **U** and $\mathbf{V}^T$ are orthogonal matrices of the singular decomposition $\mathbf{E} = \mathbf{U}\mathbf{D}\mathbf{V}^T$, $\alpha$ is a scalar, and $\mathbf{u}_3$ the third column of the matrix **U**. **W** is an orthogonal matrix defined as:

$$\mathbf{W} = \begin{bmatrix} 0 & -1 & 0 \\ 1 & 0 & 0 \\ 0 & 0 & 1 \end{bmatrix} \tag{4}$$

The choice of the true solution is determined by the condition that the points of the workspace should be in front of both cameras. This can be achieved by transforming an arbitrary point in the workspace, and determine whether it meets this condition, thus eliminating three alternatives.

## III. Retrieving R and t from a homography

A point $\mathbf{m_1}$ belonging to a plane $\pi_1$ is related to a point $\mathbf{m_2}$ belonging to another plane $\pi_2$ by [7]

$$\lambda\mathbf{m}_2 = \mathbf{H}\mathbf{m}_1 \tag{5}$$

Where $\lambda$ is a scalar showing the projective nature of the relationship, and **H** is a 3x3 matrix called homography or 2D projective transformation, is a linear transformation between points belonging to two projective planes. A special case is when one of these planes is the plane of the image. A second special case is when $\mathbf{m_1}$ and $\mathbf{m_2}$ are projections of images of a point in a plane into the scene (Fig 1). In this case **H** (homography between the planes of the images induced by the plane of the scene) is given by

$$\mathbf{H} = \mathbf{H}_{2\pi}\mathbf{H}_{1\pi}^{-1} \tag{6}$$

being $\mathbf{H}_{1\pi}$ the homography between the plane and the first image, and $\mathbf{H}_{2\pi}$ the homography between the plane and the second image.

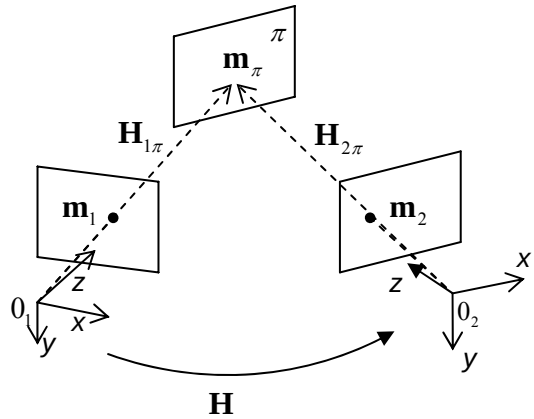


Fig. 1 System of two cameras and a plane in the scene.

In a system of two cameras, a point $\mathbf{P_1}$ with reference to three-dimensional coordinate system of the first camera can be expressed as P2 (same point, but represented in the system of the second camera) under the relation:

$$\mathbf{P}_2 = \mathbf{R}\mathbf{P}_1 + \mathbf{t} \tag{7}$$

where **R** y **t** are the rotation and translation of the system of the first camera with reference to the second camera.

If $\mathbf{P_1}$ is considered belonging to a plane in the scene, (7) can be rewritten as [7]:

$$\mathbf{P}_2 = \left(\mathbf{R} + \frac{\mathbf{t}\,\mathbf{n}_1^T}{d_1}\right)\mathbf{P}_1 \tag{8}$$

being $d_1$ the distance from the plane to the origin of coordinates of the first camera, and $\mathbf{n_1}$ is normal to the said plane. Projecting both representations of the point in each image, and using normalized coordinates ($[X / Z, Y / Z, Z / Z]^T = [u\ v\ 1]^T$ with f = 1) leads to a relationship similar to the relationship (5).

As there is a homography **H** between points belonging to the image planes of the two cameras of the form:

$$\mathbf{H} = \left(\mathbf{R} + \frac{\mathbf{t}\,\mathbf{n}_1^T}{d_1}\right) \tag{9}$$

From (9), it is possible to recover **R**, $\mathbf{n_1}$ and $\mathbf{t}/d_1$ through a process called decomposition [6]. There are several decomposition methods [6] [15] [20], we will describe briefly the method of Faugeras [6]:

Applying SVD decomposition of **H**:

$$\mathbf{H} = \mathbf{U}\mathbf{D}\mathbf{V}^T \tag{10}$$

For the general case when singular values $\sigma_1, \sigma_2$, and $\sigma_3$ of D are differents (which corresponds to a position of the plane that not contains the optical center of any camera) we have:

$$\mathbf{R} = \mathbf{U}\begin{bmatrix} \cos\theta & 0 & -\sin\theta \\ 0 & 1 & 0 \\ \sin\theta & 0 & \cos\theta \end{bmatrix}\mathbf{V}^T \tag{11}$$

ISBN: 978-607-95060-3-2
Supported by the IEEE Aguascalientes Section and the Instituto Tecnologico de Aguascalientes

$$\mathbf{t}/d_1 = (\sigma_1 - \sigma_3)\mathbf{U}(q_1, 0, q_3)^T \;;\; \mathbf{n}_1 = \mathbf{V}(q_1, 0, q_3)^T \qquad (12)$$

where

$$q_1 = \pm\sqrt{\frac{\sigma_1^2 - \sigma_2^2}{\sigma_1^2 - \sigma_3^2}} \quad \text{y} \quad q_3 = \pm\sqrt{\frac{\sigma_2^2 - \sigma_3^2}{\sigma_1^2 - \sigma_3^2}} \qquad (13)$$

and

$$\sin\theta = (\sigma_1 - \sigma_3)\frac{q_1 q_3}{\sigma_2} \quad \text{y} \quad \cos\theta = \frac{\sigma_1 q_3^2 + \sigma_3 q_1^2}{\sigma_2} \qquad (14)$$

According to the literature ([6] [18]), the decomposition produces two sets of solutions for **R t**/d1 and $\mathbf{n_1}$. Methods to rule out false solution need a priori information on the orientation of the projected plane. This paper proposes a way to discriminate the correct solution based on the dispersion of a factor that multiplies to $\mathbf{t}/\mathbf{d_1}$

*A. Discrimination of the true solution from a homography between a 3D plane and an image*

If $\beta$ is a factor that multiplies to **t*** (where $\mathbf{t}^* = \mathbf{t}/d_1$) for each point $\mathbf{m}_\pi$ in the plane and $\mathbf{m}$ is a point in the image (normalized coordinates), it holds that:

$$\lambda\mathbf{m} = \mathbf{R}\mathbf{m}_\pi + \beta\mathbf{t}^* \qquad (15)$$

in a detailed way:

$$\lambda\begin{bmatrix} u \\ v \\ 1 \end{bmatrix} = \begin{bmatrix} r_{11} & r_{12} & r_{13} \\ r_{21} & r_{22} & r_{23} \\ r_{31} & r_{32} & r_{33} \end{bmatrix}\begin{bmatrix} X \\ Y \\ 0 \end{bmatrix} + \beta\begin{bmatrix} t_x \\ t_y \\ t_z \end{bmatrix} \qquad (16)$$

where X and Y are assumed known. Multiplying and arranging terms, leads to a system:

$$\mathbf{A}\beta = \mathbf{b} \qquad (17)$$

with

$$\mathbf{A} = \begin{bmatrix} t_z u - t_x \\ t_z v - t_y \end{bmatrix}; \mathbf{b} = \begin{bmatrix} (r_{11} - r_{31}u)X + (r_{12} - r_{32}u)Y \\ (r_{21} - r_{31}v)X + (r_{22} - r_{32}v)Y \end{bmatrix} \qquad (18)$$

As (17) represents a system of two equations with one unknown, to be solved by least squares.

For each solution, n betas $\beta$ belonging to the n points in the plane are calculated. For this set of n betas $\beta$, dispersion is defined as:

$$\sigma = \sqrt{\frac{\sum_{i=1}^{n}(\beta_i - \bar{\beta})^2}{n}} \qquad (19)$$

where $\bar{\beta}$ is the average of the *n* betas $\beta$.

*B. Discrimination of the true solution from a Homography between both images*

For each point of the image1 and its corresponding point in the image2 (normalized coordinates in both images) generated from a point in a plane in the workspace, it holds that:

$$\lambda\mathbf{m}_2 = \mathbf{R}\mathbf{m}_1 + \beta\mathbf{t}^* \qquad (20)$$

(where $\mathbf{t}^* = \mathbf{t}/d_1$), in a detailed way:

$$\lambda\begin{bmatrix} u' \\ v' \\ 1 \end{bmatrix} = \begin{bmatrix} r_{11} & r_{12} & r_{13} \\ r_{21} & r_{22} & r_{23} \\ r_{31} & r_{32} & r_{33} \end{bmatrix}\begin{bmatrix} u \\ v \\ 1 \end{bmatrix} + \beta\begin{bmatrix} t_x \\ t_y \\ t_z \end{bmatrix} \qquad (21)$$

multiplying and arranging terms leads to a system of the form (17) with:

$$\mathbf{A} = \begin{bmatrix} t_z u' - t_x \\ t_z v' - t_y \end{bmatrix}$$
$$\mathbf{b} = \begin{bmatrix} (r_{11} - r_{31}u')u + (r_{12} - r_{32}u')v + (r_{13} - r_{33}u') \\ (r_{21} - r_{31}v')u + (r_{22} - r_{32}v')v + (r_{23} - r_{33}v') \end{bmatrix} \qquad (22)$$

Just as in the previous case, $\beta$ is calculated for each point by least squares, the dispersion is calculated for each solution and applies the criterion of minimum dispersion to the true solution

## IV. Experiments

*A. Equipment used*

The equipment used is as follows (Fig. 2):

A joint system consists of a high-precision positioning and its driver, model MM3000 Newport. It has three degrees of freedom: two axes of rotation and an axis of translation and its theoretical accuracy is one thousandth of a degree and a thousandth of an mm. On the last link of the joint system is arranged the visual object to be reconstructed, formed by a plane containing 25 black squares on a white background.

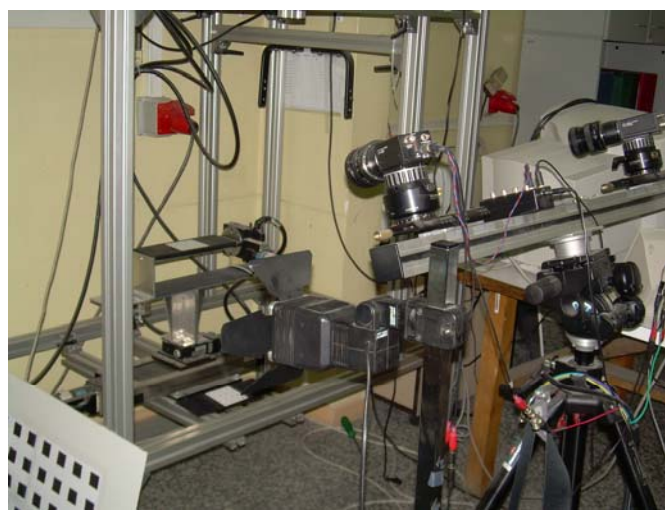

Fig. 2 Experimental equipment.

A vision system consisting of two analog CV-M50 cameras and a Meteor Matrox II-MC image acquisition card, which allows the simultaneous acquisition of both images. The cameras, fixed in the workspace, separated approximately 700 mm, converging towards the joint system at a distance about 1200 mm. The detection of the characteristics is with subpixel precision, and with an error less than 0.2 pixels

ISBN: 978-607-95060-3-2
Supported by the IEEE Aguascalientes Section and the Instituto Tecnologico de Aguascalientes

*B. Tests realized*

Assuming that the intrinsic parameters of both cameras are known, as well as weak calibration of the system (fundamental matrix **F**) obtained by the method of the eight points [11] with normalization of input data.

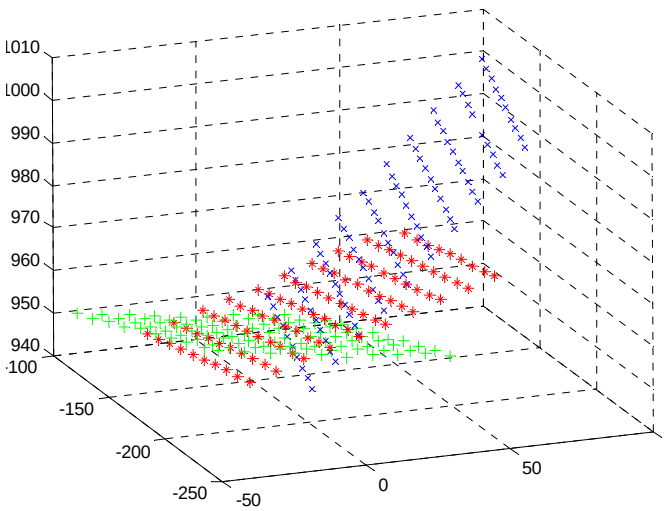


Fig. 3 3D Reconstruction with true **R** and **t**.

In order to serve as a framework, the true rotation matrix **R** and translation vector **t** between the two cameras are determined before tests. These parameters can be obtained by two methods. The first is through:

$$\begin{bmatrix} \mathbf{R} & \mathbf{t} \\ \mathbf{0}^T & 1 \end{bmatrix} = \begin{bmatrix} \mathbf{R}_{2\pi} & \mathbf{t}_{2\pi} \\ \mathbf{0}^T & 1 \end{bmatrix} \begin{bmatrix} \mathbf{R}_{1\pi} & \mathbf{t}_{1\pi} \\ \mathbf{0}^T & 1 \end{bmatrix}^{-1} \tag{23}$$

where $\mathbf{R}_{1\pi}$ and $\mathbf{t}_{1\pi}$ are elements of the pose between the pattern system and the first camera, obtained relating the spatial positions of the corners of the pattern and their image projections in the first camera, by similar process was obtained $\mathbf{R}_{2\pi}$ and $\mathbf{t}_{2\pi}$ relating the 3D positions of the corners of the pattern with their image projections in the second camera. The second method is the method of Horn [14] from the equation of the motion of the rigid body (7) minimizes the expression:

$$\sum_i^n \left\| \mathbf{P}_{2i} - (\mathbf{R}\mathbf{P}_{1i} + \mathbf{t}) \right\|^2 \tag{24}$$

where $\mathbf{P}_1$ and $\mathbf{P}_2$ are 3D points belonging to the camera system 1 and 2 respectively. In this work, **R** and **t** have been obtained through the first method.

The tests carried out were three-dimensional reconstruction of the corners of 25 black squares belonging to the pattern whose image is acquired at different positions by both cameras, so that the optical center of any of them does not belong to the plane of the pattern to avoid singularities. 3D reconstructions (Euclidean) of these corners using real rotation and translation using the method of minimizing the reprojected rays [13] and eliminating distortion in detecting characteristics serve as reference for calculation errors. Figure 3 shows the 3D reconstruction of three positions of the pattern.

Subsequently, the 3D reconstruction of the corners detected is carried out using the **R** and **t** retrieved from: a) the homography generated by the points belonging to the flat pattern (Fig. 4), b) the fundamental matrix **F** of the system. Reconstruction is done in three situations: 1) eliminating image distortion of the detected points, 2) without eliminating the distortion of the detected points, and 3) by adding Gaussian noise (without eliminating the distorting) $\sigma = 0.5$ or $\sigma = 1$ pixels to the detected characteristics. It is measured the average Euclidean error (in pixels) between the reprojection in the image of the real 3D reconstructed points and those reconstructed with the recovered rotation and translation (expression (25)). Since there are two images, the calculated error is the average of the errors in both images

$$e = \frac{1}{n} \sum_i^n \left\| \mathbf{m}_i^* - \mathbf{m}_i \right\| \tag{25}$$

Fig. 4 shows the 3D reconstruction with **R** and $\beta\mathbf{t}^*$ (where $\mathbf{t}^* = \mathbf{t}/d_1$) retrieved from a homography **H** for an arbitrary value of $\beta$. High distortion of the point reconstructed is observed (compare with Fig. 3).

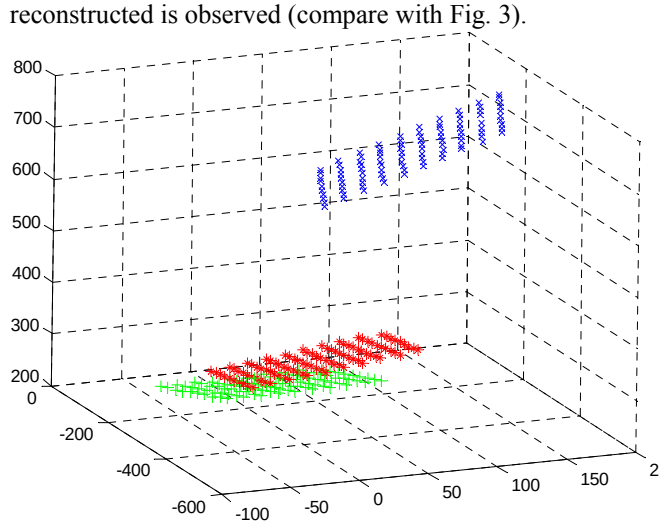


Fig. 4 3D reconstruction utilizing **R** and **t** retrieved from a homography **H** for an arbitrary value of $\beta$.

Errors generated by the 3D reconstruction with **R** y $\beta\,\mathbf{t}^*$ (from a homography, $\mathbf{t}^* = \mathbf{t}/d_1$) or **R** and $\alpha\,\mathbf{t}^*$ (from the fundamental matrix, $\mathbf{t}^* = \alpha\mathbf{u}_3$) are calculated for different values of $\beta$ (o $\alpha$). Graphs of Fig. 5-8 are obtained, these graphs depicts the error (vertical axis) VS the product between $\beta$ **(o** $\alpha$ **)** and the norm of **t*** (horizontal axis)

$$\beta\|\mathbf{t}^*\| \quad \text{ó} \quad \alpha\|\mathbf{t}^*\| \tag{1}$$

Figure 5 shows results for the recovery from the homographies of 3 positions of the pattern, and from the fundamental matrix, eliminating the image distortion case. Figure 6 shows the same situation but without the

ISBN: 978-607-95060-3-2
Supported by the IEEE Aguascalientes Section and the Instituto Tecnologico de Aguascalientes

elimination of the distortion case. Comparing Fig 5 and Fig 6, lower values of error for eliminating image distortion case are showed.

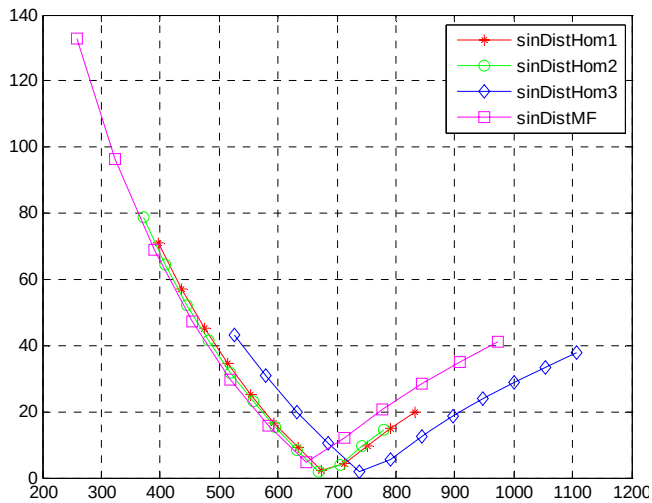


Fig. 5 Reprojection error when image distortion is eliminated.

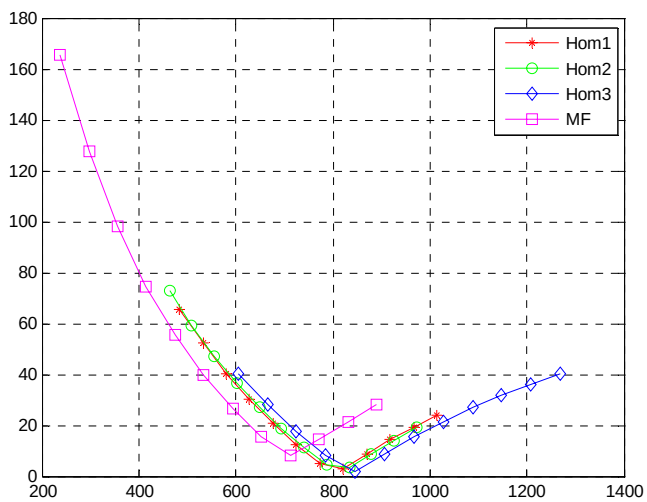


Fig. 6 Reprojection error when image distortion is not eliminated.

Results for the cases when Gaussian noise is added to the detection of features, are shown in Figure 7 and Figure 8 respectively.

## V. Results

According to figures 5-8, a parabolic behavior of the error increasing downward away from the optimum value of $\beta\|\mathbf{t}^*\|$ or ($\alpha\|\mathbf{t}^*\|$) is showed.

Based on Fig 5 and 6 are obtained Table I and based on Figs 7 and 8 Table II that show the minimum error and its corresponding $\beta\|\mathbf{t}^*\|$ for homographies of three positions of the pattern.

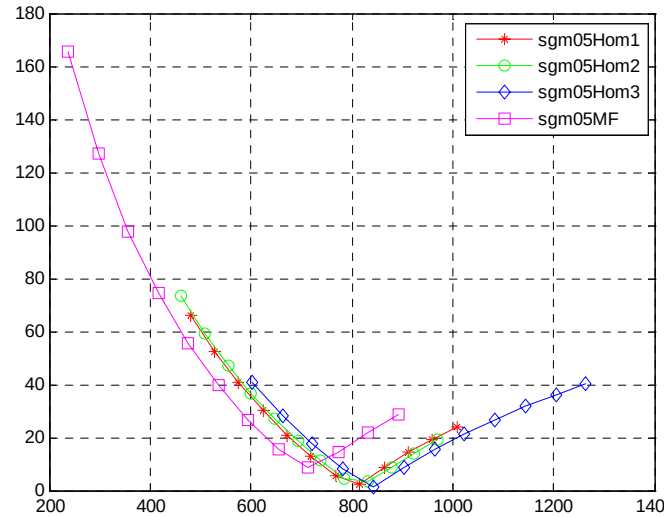


Fig. 7 Reprojection error with added noise $\sigma = 0.5$.

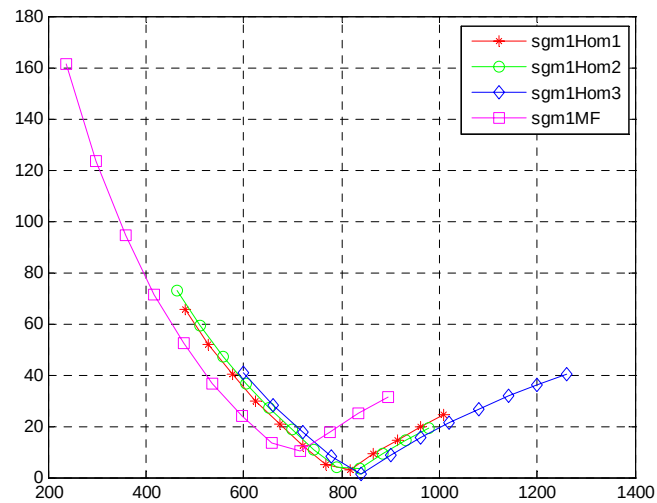


Fig. 8 Reprojection error with added noise $\sigma = 1$.

TABLE I
MINIMUM ERROR AND $\beta\|\mathbf{t}^*\|$ FROM HOMOGRAPHIES WITH DISTORTION CORRECTED AND WITHOUT CORRECTED

| Distortion | Parameters | $\mathbf{H}_1$ | $\mathbf{H}_2$ | $\mathbf{H}_3$ |
|---|---|---|---|---|
| corrected | $e_{min}$ | 2.2 | 1.8 | 1.8 |
| | $\beta\|\mathbf{t}^*\|$ | 673.1 | 668.8 | 737.9 |
| without corrected | $e_{min}$ | 5.1 | 3.2 | 1.6 |
| | $\beta\|\mathbf{t}^*\|$ | 773.6 | 833.4 | 845.9 |

TABLA II
MINIMUM ERROR AND $\beta\|\mathbf{t}^*\|$ FROM HOMOGRAPHIES WITH ADDED NOISE

| Noise | Parameters | $\mathbf{H}_1$ | $\mathbf{H}_2$ | $\mathbf{H}_3$ |
|---|---|---|---|---|
| $\sigma = 0.5$ | $e_{min}$ | 2.6 | 3.2 | 1.5 |
| | $\beta\|\mathbf{t}^*\|$ | 815.8 | 831.4 | 842.8 |
| $\sigma = 1$ | $e_{min}$ | 3.0 | 3.4 | 1.5 |
| | $\beta\|\mathbf{t}^*\|$ | 817.3 | 837.6 | 840.6 |

ISBN: 978-607-95060-3-2
Supported by the IEEE Aguascalientes Section and the Instituto Tecnologico de Aguascalientes

Given that the true value of the translation **t** (665.5) is known, which serves as a reference, and comparing with the values of Tables I, it is seen that values closer to the reference are obtained when distortion is corrected, this fact shows a significant dependence of the result to the correction of the distortion in cameras. Comparing with Table II, the added noise does not degrade to a large extent the result when the distortion is not corrected. Moreover, the results for cases with added noise $\sigma = 0.5$ and $\sigma = 1$ are very similar.

In the case of recovery from the fundamental matrix (Table III) shows a good result when you delete the image distortion, while the results are very similar to each other (although not very far from the reference value) when distortion is not removed or Gaussian noise is added. It is also noted that the minimum error values are much larger than in the case of recovery from the homographies (Tables I and II), which represents a worst estimate of the rotation R recovered in the case from homographies.

TABLA III
MINIMUM ERROR AND $\alpha\|\mathbf{t}^*\|$ FROM THE FUNDAMENTAL MATRIX

| Parameters | without distortion | with distortion | $\sigma = 0.5$ | $\sigma = 1$ |
|---|---|---|---|---|
| $e_{min}$ | 4.6 | 8.4 | 8.7 | 10.5 |
| $\alpha\|\mathbf{t}^*\|$ | 648.6 | 712.5 | 713.4 | 716.1 |

## V. CONCLUSION

The recovery of the rotation **R** and translation **t** between the coordinate systems of cameras in a stereo system with two cameras was performed. This recovery was carried out from homographies which is generated by a flat pattern in the scene and from the epipolar geometry of the system represented by the fundamental matrix **F**. In both cases, the translation **t** is recovered with a factor due to the projective nature of the system. It is shown that both in the case of recovery from homography as in the case of recovery from the fundamental matrix, we obtain good results if the distortion of the cameras is corrected. It is also observed that both cases are robust to the addition of noise. We also observe that fewer errors are obtained when recovery is realized from homographies

As future work it is desired to obtain optimal values $\beta\|\mathbf{t}^*\|$ and $\alpha\|\mathbf{t}^*\|$ not dependent of the previous estimation of true 3D points. It is also proposed to extend this study to a system of three cameras and knowledge of the trifocal tensor.

## REFERENCES

[1] Adachi J., and Sato J. "Uncalibrated Visual Servoing from Projective Reconstruction of Control Values". Proceedings of the 17th Int. Conf. on Pattern Recognition (ICPR'04).
[2] Chaumette F. and Hutchinson S. "Visual Servo Control Part I: Basic Approaches". IEEE Robotics & Automation Magazine, vol.14, issue 1, pp. 109-118, 2006.
[3] Chesi G., Prattichizzo D., and Vicino A. "A Visual Servoing Algorithm based on Epipolar Geometry". International Conference on Robotics & Automation. Seoul Korea May21-26, 2001.
[4] Deguchi K. "Optimal Motion Control for Image-Based Visual Servoing by Decoupling Translation and Rotation". IEEE/RSJ Int. Conference on Intelligent Robots and Systems, Victoria B.C., Canada, October 1998.
[5] Espiau B., Chaumette F., and Rives P. "A New Approach to Visual Servoing in Robotics". IEEE Transactions on Robotics and Automation, 8(3), pp. 313-326, 1992.
[6] Faugeras, O., and Lustman, F. "Motion and Structure From Motion in a Piecewise Planar Environment". Int. Journal on Pattern Recognition and Artificial Intelligence, 2(3), pp. 485-508, 1988.
[7] Faugeras O, Three-Dimensional Computer Vision. The Massachusetts Institute of Technology Press, 1993.
[8] Faugeras O., and Luong Q.T. "The Geometry of Multiple Images". The Massachusetts Institute of Technology Press, 2001.
[9] Hanning T., Graf S., and Kellner M. "Re-projective VS Projective Camera Calibration: Effects on 3D-Reconstruction". IEEE International Conference on Image Processing ICIP 2005, 11-14 Sept. 2005.
[10] Hartley, R.I. "Estimation of Relative Camera Position for Uncalibrated Cameras". European Conference on Computer Vision. LNCS vol. 588, pp. 579-587,1992.
[11] Hartley, R.I.. "In Defence of the Eight-Point Algorithm". IEEE Transactions on Pattern Analysis and Machine Intelligence, Vol. 19, Nº 6, June, 1997.
[12] Hartley R., and Zisserman A. Multiple View Geometry in Computer Vision. 2nd Ed., Cambridge University Press, 2003.
[13] Hartley R., and Sturn P "Triangulation". Computer Vision and Image Understanding. Vol. 68 Nº 2, pp. 146-157, November 1997.
[14] Horn, B.K.P., Hilden, H.M., Negahdaripour, S. *Close-Form Solution of Absolute Orientation Using Orthonormal Matrices*. J. Opt. Soc. Am. Ser. A 5: 1127-1135. 1988
[15] Ma, Y., Soatto, S., Kosecka, J., and Sastry, S.S. An Invitation to 3-D Vision: From Images to Geometric Models. New York: Springer-Verlag Inc., 2004.
[16] Rothwell Ch., Csurka G., and Faugeras O. "A Comparison of Projective Reconstruction Methods for Pairs of Views". Rapport of Recherche Nº 2538, INRIA Sophia-Antípolis, 1995.
[17] Solanski S.C., Dixon W.E., Crane C.D., and Gupta S. "Uncalibrated Visual Servo Control of Robot Manipulators with Uncertain Kinematics". 45th IEEE Conference on Decision & Control, San Diego, CA, USA, December 13-15, 2006.
[18] Vargas M. and Malis E. "Visual Servoing Based on an Analytical Homography Decomposition". 44th IEEE Conference on Decision and Control, and the European Control Conference 2005, Seville, Spain, December 12-15, 2005.
[19] Zhang Z. "Determining the Epipolar Geometry and its Uncertainty: A review". International Journal of Computer Vision 27(2), 161-195, 1998.
[20] Zhang Z., and Hanson A.R. "Scaled Euclidean 3D Reconstruction based on Externally Uncalibrated Cameras". IEEE Symposium on Computer Vision, Coral Gables, Florida, 1995.

ISBN: 978-607-95060-3-2
Supported by the IEEE Aguascalientes Section and the Instituto Tecnologico de Aguascalientes